Spark plasma sintering of ZrB_2-ZrC powder mixtures synthesized by MA-SHS in air

Takeshi Tsuchida* and Satoshi Yamamoto

Division of Materials Science and Engineering, Graduate School of Engineering, Hokkaido University, N13 W8, Kita-ku, Sapporo, 060-8628, Japan

Abstract

Mechanical activation assisted self-propagating high-temperature synthesis (MA-SHS) in air was successfully applied to the synthesis of the powder mixtures of ZrB_2 and ZrC as a precursor of the ZrB_2-ZrC composite. When the powder mixtures of Zr/B/C=4/2/3~6/10/1 in molar ratio were mechanically activated (MA) by ball milling for 45-60 min and then exposed to air, they self-ignited spontaneously and the self-propagating high-temperature synthesis (SHS) was occurred to form ZrB_2 and ZrC. The ZrB_2-ZrC composites were produced from these MA-SHS powders by spark plasma sintering (SPS) at 1800ºC for 5-10 min and showed the fine and homogeneous microstructure composed of the < 5 μm-sized grains. The mechanical properties of the composites evaluated by Vickers indentation method showed the values of Vickers hardness of 13.6~17.8 GPa and fracture toughness of 2.9~5.1 $MPa \cdot m^{1/2}$, depending on the molar ratio of ZrB_2/ZrC. Thus, the better microstructure and mechanical properties of the ZrB_2-ZrC composites were obtained from the MA-SHS powder mixtures, compared with those obtained from the MA powder, the mixing powder and the commercial powder mixtures.

Keywords:

Mechanical activation (MA); Self-propagating High-temperature Synthesis (SHS); Spark plasma sintering (SPS); Ball milling; ZrB_2-ZrC composite; Zr/B/C powder mixtures,

*Corresponding author: Takeshi Tsuchida

Tel/Fax: +81 11 706 6578

e-mail address: tsuchida@eng.hokudai.ac.jp

1. Introduction

Boride and carbide of zirconium show a number of excellent properties such as high melting temperature, high strength, high thermal and electrical conductivity, and chemical stability. Therefore, the use of these ceramics in composites can be expected to offer potential candidates for a variety of high-temperature structural applications [1-4]. Actually, the mechanical properties of the composites, such as mechanical strength, hardness and fracture toughness are controlled by densification and microstructure of the sintered bodies. In particular, because it is known that ceramic materials with fine microstructures, especially nanocomposites, exhibit improved mechanical properties [5], the preparation of the powder mixtures of ZrB_2 and ZrC with fine, homogeneous microstructure is definitely important. We have so far developed mechanical activation assisted self-propagating high-temperature synthesis (MA- SHS) in air, and successfully applied to the synthesis of carbides and nitrides of Al, Zr and Nb [6-12], and borocarbides of Al_3BC [13]. This technique is based on SHS induced by self-ignition reaction of disordered carbon when the mechanically activated metal-graphite powder mixtures were exposed to air [6,8]. Thus, this process does not need any expensive reaction equipments and is a very simple, energy-saving technique. We have reported that using this MA-SHS process, the powders of ZrB_2 and ZrC with fine, homogeneous microstructure were synthesized from the powder mixture of Zr/B/C=1/1/1, and they are expected to be a promising candidate as precursor of the ZrB_2- ZrC composites [14].

On the other hand, there is another problem that the sintering of ZrB_2 and ZrC powders to form the composite is a difficult process because of the high melting point and high vapor pressure of the constituents. Spark plasma sintering (SPS) is one of the most powerful candidates to densify poorly sinterable materials such as ZrB_2 and ZrC. SPS is a noble sintering process that allows compaction of ceramic powders at very lower temperature with shorter holding time than in more conventional sintering process. The sample is loaded in a graphite die, uniaxial pressure is applied during the sintering by the top and bottom punches, and a pulsed direct current is allowed to pass through the die and the sample. The pulses generate spark discharge and/or plasma between powder particles. Because the die acts also as a heating source, the sample is effectively heated from both outside and inside. Although the mechanism for densification and grain growth in the SPS process have not been well elucidated yet, Tokita [15] pointed out that the generated spark discharge and/or plasma cleans the surfaces from adsorbed species, such as CO_2, H_2O, OH^-, so that enhances the

grain-boundary diffusion process for densification. A systematic study of various spark plasma sintering (SPS) parameters, namely temperature, holding time, heating rate, pressure, and pulse sequence was conducted by Shen et al. [16] in order to investigate their effect on the densification, grain-growth kinetics, hardness, and fracture toughness of a commercially available submicrometer-sized Al_2O_3 powder.

In the present study, we have synthesized the powder mixtures of ZrB_2 and ZrC by the useful MA-SHS process in air from the powder mixtures with various molar ratios of Zr/B/C=4/2/3~6/10/1, sintered them by SPS to obtain the ZrB_2-ZrC composites and characterized their mechanical properties such as Vickers hardness and fracture toughness.

2. Experimental procedures

The powders of zirconium metal (particle size of less than 150 μm, 98% purity, Kojundo Chemical Laboratory), amorphous boron (practical grade, Sigma Chemical Company) and natural graphite (mean flake size 5 μm, 97% carbon, 2% ash and 1% volatile component, Nippon Kokuen Industry) were used as starting materials. The particle size and morphology of these materials has been previously described [14]. The powders were mixed in various molar ratios of Zr/B/C=4/2/3~6/10/1 in an agate mortar, loaded in a p-7 planetary ball mill (Fritsch, Idar-Oberstein, Germany) in air and then ground for 45~60 min. A 25 ml jar and seven balls of 12 mm in diameter of tungsten carbide were used for grinding. The amount of powder mixture loaded was 6.0-10.8 g, and the weight ratio of powder to balls was about 1:15-1:8.5. The grinding was interrupted every 15 min, and the sample was scraped from the balls and the sidewalls of the jar and then reloaded to continue grinding. After grinding, the ground sample was transferred into a graphite crucible (inner diameter of 30 mm and depth of 40 mm) and exposed to air. Just then, it self-ignited and the exothermic reactions propagated into the reactant powders. As soon as the reactions started, the graphite crucible was covered with another one to prevent the sample from further oxidizing. After the reaction, a swelled lump of the product formed and a small amount of the unreacted sample remained in a crucible. The product was ground in an agate mortar and then subjected to the following experiments.

The obtained powder mixtures were wrapped in graphite foil of 0.2 mm thick, loaded in a graphite die (10 mm in diameter) and spark plasma sintered at 1800ºC for 5-10 min under a

vacuum of 6-10 Pa with SPS apparatus (SPS-510L, Sumitomo Coal Mining Co., Tokyo, Japan). The temperature was measured with an optical pyrometer focused on the surface of the graphite die and automatically heated from room temperature to 600ºC at heating rate of 120ºC min^{-1} and then up to 1800ºC at 40ºC min^{-1}. A pressure of 40 MPa and an on-off pulse sequence of 12:2 were applied to the sample during entire sintering time. At the end of the holding time, the pressure was released and the current was shut off. For the comparison, the following samples were also sintered by SPS: the powder mixture of Zr/B/C=2/2/1 which was mechanically activated for 45 min, but exposed to air after being left for 24 h in the jar to prevent self-ignition (which is called as MA sample); the powder mixture of Zr/B/C=2/2/1 which was merely mixed in an agate mortar without mechanical activation (which is called as mixing sample); the powder mixture of ZrB_2/ZrC=1/1, which was obtained by mixing the commercially available samples in an agate mortar (which is called as commercial sample). The purity of the commercial ZrB_2 and ZrC powders was 97 and 95% (Kojundo Chemical Laboratory), respectively and their particle size was a few ~ 10 μm by SEM observation (Fig.2(c), (d)).

The density of the sintered bodies was measured by Archimedes method. Before X-ray diffraction (XRD) and scanning electron microscopy (SEM), and the hardness and toughness measurements, the surface of the sintered samples was mirror-like polished with 1.0 μm diamond slurries and when needed, etched chemically in a solution of 6N HCl at room temperature for 5 h. The crystalline phases were detected by XRD (RINT-2000, Rigaku Denki) using Ni-filtered CuKα radiation (30 kV, 15 mA). The microstructures were observed on the polished surfaces and the fracture surfaces with scanning electron microscopy (JSM-5410-SEM-EPMA-WDX combined microanalyzer, JEOL). For the SEM observation of the ground samples and the commercial samples, the powder sample was dispersed in ethanol by ultrasonication, and was placed as a drop on a glass plate or a brass stub and then dried.

The Vickers hardness (HV) and fracture toughness (K_C) at room temperature were evaluated by Vickers indentation technique at a load of 4.9 MPa. More than five indents were made at the middle of each sample. The fracture toughness was calculated according to JIS R1607 [17], $K_C = 0.026(E^{1/2}P^{1/2}a/C^{3/2})$, where P is the indentation load, a the half-length of the indent, C the half-length of the crack, and E the Young's modulus of the composite. The Young's modulus value of 435 GPa was used as the mean of 470 GPa for ZrB_2 and 400 GPa for ZrC.

3. Results and discussion

The reaction mechanism of MA-SHS process in air for the formation of ZrB_2 and ZrC from the powder mixture of Zr/B/C=1/1/1 has already discussed in the previous paper [14]. In the MA-SHS process in air, it was found to be essential that graphite is converted into finely divided, disordered carbon by mechanical activation and mixed with the finely ground particles of Zr and B in an intimate contact state. Fig.1 shows the X-ray diffraction patterns of the MA-SHS powders obtained from the different powder mixtures of Zr/B/C=4/2/3~6/10/1, these ratios corresponding to the molar ratios of ZrB_2/ZrC=1/3~5/1, shown in the parentheses, expected as the product phases. After the grinding of 45~60 min, all the powder mixtures self-ignited in air and the subsequent exothermic reaction violently occurred evolving white heat. The radiance due to this SHS reaction increased with the boron content in the Zr/B/C powder mixtures. This results from the evolution of the formation enthalpy of ZrB_2, ca. -320 kJ mol^{-1} larger than that of ZrC, ca. -200 kJ mol^{-1} in the temperature range of 300-1500ºC. After the reaction, as shown in Fig.1 only hexagonal ZrB_2 and cubic ZrC phases were obtained, and the intensity ratio of ZrB_2/ZrC changed in accordance with the ratios of ZrB_2/ZrC=1/3~5/1 expected from the molar ratio of Zr/B/C=4/2/3~6/10/1 in the reactants.

Fig. 2 shows the optical and SEM microphotographs of the ZrB_2 and ZrC samples obtained by MA-SHS in the powder mixture of Zr/B/C=2/2/1 and the commercially available samples. After the MA-SHS process, as shown in Fig.2(a), the product was obtained in a morphology of the swelled and stratified structure. A formation mechanism of such a unique morphology has been discussed in the previous paper [11] on the basis of the unstable combustion reaction. At only the outermost layer of the product, corresponding to the left-handed surface of the lump in the figure, ZrO_2 was detected as a main phase. Hence its layer was removed, the remaining product lump was ground in an agate mortar, and then was subjected to XRD (Fig.1) and SEM (Fig.2(b)). In addition, the presence of amorphous boron and disordered carbon, unreacted Zr and ZrO_2 was not detected by Raman spectroscopy for the MA-SHS powders of Zr/B/C=3/2/2, 2/2/1 and 3/4/1, indicating the product being ZrB_2 and ZrC phases exclusively. It can be seen in Fig.2(b) that the powder mixtures of ZrB_2 and ZrC obtained are consisted of the particles from submicrometer to 5 μm. The similar results were obtained in other samples with different molar ratios of Zr/B/C. On the other hand, as shown in Figs.2(c) and 2(d), the commercially available samples of ZrB_2 and ZrC were

consisted of < 10 μm-sized particles, in particular ZrB_2 grains showed clear-cut surfaces.

Fig.3 shows the SEM microphotographs of the ZrB_2-ZrC compacts sintered by SPS from different samples, namely, the MA-SHS powder, the MA powder, the mixing powder and the commercial powder at 1800ºC for 5-10 min under a vacuum of 6-10 Pa. According to EPMA observation, the light phase is ZrC and the grey phase is ZrB_2. Among these compacts, the much fine, homogeneous microstructure can be seen for the MA-SHS powder compact in Fig.3(a). The grain size of ZrB_2 and ZrC is almost < 5 μm and is equivalent to the particle size of the starting powders shown in Fig,2(b), indicating retardation of grain growth during SPS process. In contrast, the other compacts in Fig.3(b)-(d) showed the agglomeration of somewhat larger grains than those in Fig.3(a). Particularly, the slightly heterogeneous microstructure containing the grain > 10 μm was observed in the commercial powder compact in Fig.3(d). The relative density and the mechanical properties of Vickers hardness, HV and fracture toughness, K_C of these compacts are summarized in Table 1. The ZrB_2-ZrC composite compact obtained from the MA-SHS powder showed the high relative density of 98.5 %, the Vickers hardness of 17.8 GPa and the fracture toughness of 3.8 $MPa \cdot m^{1/2}$, whereas the other three compacts showed the lower relative density of 96.9-97.6 %, the Vickers hardness of 13.7-16.6 GPa and the fracture toughness of 3.4-4.5 $MPa \cdot m^{1/2}$, respectively. It can be easily assumed that the sintering behavior and the densification rate strongly depend on the reactivity of the starting powder, such as particle size, specific surface area, surface defect structure and so on. Therefore, the better values of hardness and fracture toughness of the MA-SHS powder compact seem to primarily depend on its smaller grain size and homogeneous microstructure. The similar hardness-grain size dependence has been obtained by Shen [16], and Krell and Blank [18], and considered to ascribe to the limited mobility of dislocation in small grains. In addition, it was found from the SEM observation of the fracture surfaces that many cracks were deflected at the grain boundaries, which would lead the increase in the fracture toughness. To discuss on the hardness and/or fracture toughness-grain size dependence in detail, the study about the interface structure between ZrB_2 and ZrC grains and the dislocation behavior by high resolution TEM is very interesting.

Fig.4 shows the SEM microphotographs of the SPS compacts obtained from the MA-SHS powders of Zr/B/C=4/2/3~5/8/1. The relative density and mechanical properties of HV and K_C of these compacts are summarized in Table 2. Depending on the Zr/B/C ratio, the difference in the dispersion and aggregation of ZrB_2 (grey phase) and ZrC (light phase) grains

can be seen in the figure. That is, with increasing in boron content the growth of ZrB_2 grain and the increase in porosity is noticeable. In fact, the relative density of the SPS compact of Zr/B/C=5/8/1, corresponding to the ratio of ZrB_2/ZrC=4/1, was 97.5 %. Similar tendency can be also admitted in the compacts with increased carbon content. Thus, depending on the ratio of ZrB_2/ZrC, ZrB_2 or ZrC phase becomes secondary-phase particle or matrix, and consequently the mechanical properties of the composites are influenced. In general, the ZrC rich compacts obtained from the Zr/B/C=4/2/3 and 3/2/2 powder mixtures showed higher values of HV and lower values of K_C. Inversely, the ZrB_2 rich compacts obtained from the Zr/B/C=3/4/1, 4/6/1 and 5/8/1 powder mixtures posses the lower HV and higher K_C. This tendency of the mechanical properties of the composites seems to reflect the properties of matrix phase, that is, ZrB_2 posses the HV, ~22 GPa lower than 25~26 GPa of ZrC and K_C, 4-5 $MPa \cdot m^{1/2}$ higher than 2.8 $MPa \cdot m^{1/2}$ of ZrC. Totally, the ZrB_2-ZrC composite obtained from the MA-SHS powder of Zr/B/C=2/2/1 showed better values of HV and K_C as the average of the properties for both ZrB_2 and ZrC phases. For the comparison, the single phase of ZrB_2 and ZrC commercial powder was also SPS-sintered at 1800ºC for 10-20 min under a vacuum of 6-10 Pa, respectively. However, the relative density obtained was 84.7 % for ZrB_2 compact and 88.3 % for ZrC compact, these values were too low to measure HV and K_C. Therefore, the higher sintering temperature of 2000ºC or above is needed to obtain the dense ZrB_2 and ZrC sintered bodies, respectively.

In conclusion, it was verified that the MA-SHS process in air is an unique and energy-saving technique to synthesize concurrently the ZrB_2 and ZrC powders with fine and homogeneous microstructure. Then, using the MA-SHS powder mixtures the ZrB_2-ZrC composites with a fine and homogeneous microstructure and better mechanical properties were able to be obtained by SPS technique at a temperature as low as 1800ºC. The values of Vickers hardness HV of 13.6~17.8 GPa and fracture toughness K_C of 2.9~5.1 $MPa \cdot m^{1/2}$ of these composites were obtained depending on the molar ratio of Zr/B/C in the starting materials. From these results, we can select the desired ZrB_2-ZrC composite with the desired mechanical properties. In addition, it would be possible to synthesize the nanocomposite of ZrB_2-ZrC, when the powders consisted of nanosized particles were available as a starting powder. The study of crystallographic orientation of ZrB_2/ZrC phase boundary and plastic deformation mechanism associated with the dislocation motion is also a fascinating following theme.

Acknowledgement

The authors gratefully acknowledge support for this research by a Grant-in Aid for Scientific Research (C) (KAKENHI 14550797)) and by Nippon Sheet Glass Foundation for Materials and Engineering, and also the help received from Dr. K. Kurokawa with SPS experiments.

References

[1] W.B.Johnson, A.S.Nagelberg, and E.Breval, J.Am.Ceram.Soc. **74**(9), (1991) 2093.

[2] E.Breval, and W.B.Johnson, J.Am.Ceram.Soc. **75**(8), (1992) 2139.

[3] S.H.Shim, K.Niihara, K.H.Auh, and B.Shim, J.Microscopy. **205**(3), (2002) 238.

[4] K.Kuwabara, Ceramics Jpn. **37**(4), (2002) 267.

[5] K.Niihara, J.Ceramic.Soc.Jpn. **99**(10), (1991) 974.

[6] T.Tsuchida, T.Hasegawa, and M.Inagaki, J.Am.Ceram.Soc. **77**(12), (1994) 3227.

[7] T.Tsuchida, T.Kitagawa, and M.Inagaki, Eur.J.Solid State Inorg.Chem. **32** (1995) 629.

[8] T.Tsuchida, and T.Hasegawa, Thermochim. Acta. **276** (1996) 123.

[9] T.Tsuchida, T.Hasegawa, T.Kitagawa, and M.Inagaki, J.Eur.Ceram.Soc. **17** (1997) 1793.

[10] T.Tsuchida, T.Kitagawa and M.Inagaki, J.Mater.Sci. **32** (1997) 5123.

[11] T.Tsuchida, M.Kawaguchi, K.Kodaira, Solid State Ionics. **101-103** (1997) 149.

[12] T.Tsuchida, and Y.Azuma, J.Mater.Chem. **7**(11), (1997) 2265.

[13] T.Tsuchida, and T.Kan, J.Eur.Ceram.Soc. **19** (1999) 1795.

[14] T.Tsuchida, and S.Yamamoto, J.Eur.Ceram.Soc. **24** (2004) 45.

[15] M.Tokita, J.Soc.Powder Technol. Jpn. **30** (1993) 790.

[16] Z.Shen, M.Johnsson, Z.Zhao, and M.Nygren, J.Am.Ceram.Soc. **85** (2002) 1921.

[17] Japanese Industrial Standard No. JIS R 1607, Testing methods for fracture toughness of fine ceramics, 1995, p.1.

[18] A.Krell, and P.Blank, J.Am.Ceram.Soc. **78**[4], (1995) 1118.

Figure captions

Fig.1 The XRD patterns of the MA-SHS powders obtained from the different powder mixtures of Zr/B/C=4/2/3~6/10/1, these ratios correspond to the ratios of ZrB_2/ZrC=1/3~5/1, shown in the parentheses, expected as the product phases

Fig.2 (a) The optical microphotographs of the product lump obtained by MA-SHS from the powder mixture of Zr/B/C=2/2/1, and SEM microphotographs of (b) the ZrB_2 and ZrC powder mixtures obtained by grinding the lump in an agate mortar, which XRD pattern is shown in Fig.1, and the commercial powders of (c) ZrB_2 and (d) ZrC

Fig.3 The SEM microphotographs of the ZrB_2-ZrC composite sintered by SPS from different samples, (a) the MA-SHS powder, (b) the MA powder, (c) the mixing powder and (d) the commercial powder, which are described in detail in text, at 1800ºC for 5-10 min under a vacuum of 6-10 Pa

Fig.4 The SEM microphotographs of the ZrB_2-ZrC composite sintered by SPS from the different MA-SHS powders of Zr/B/C=4/2/3~5/8/1

Fig.1

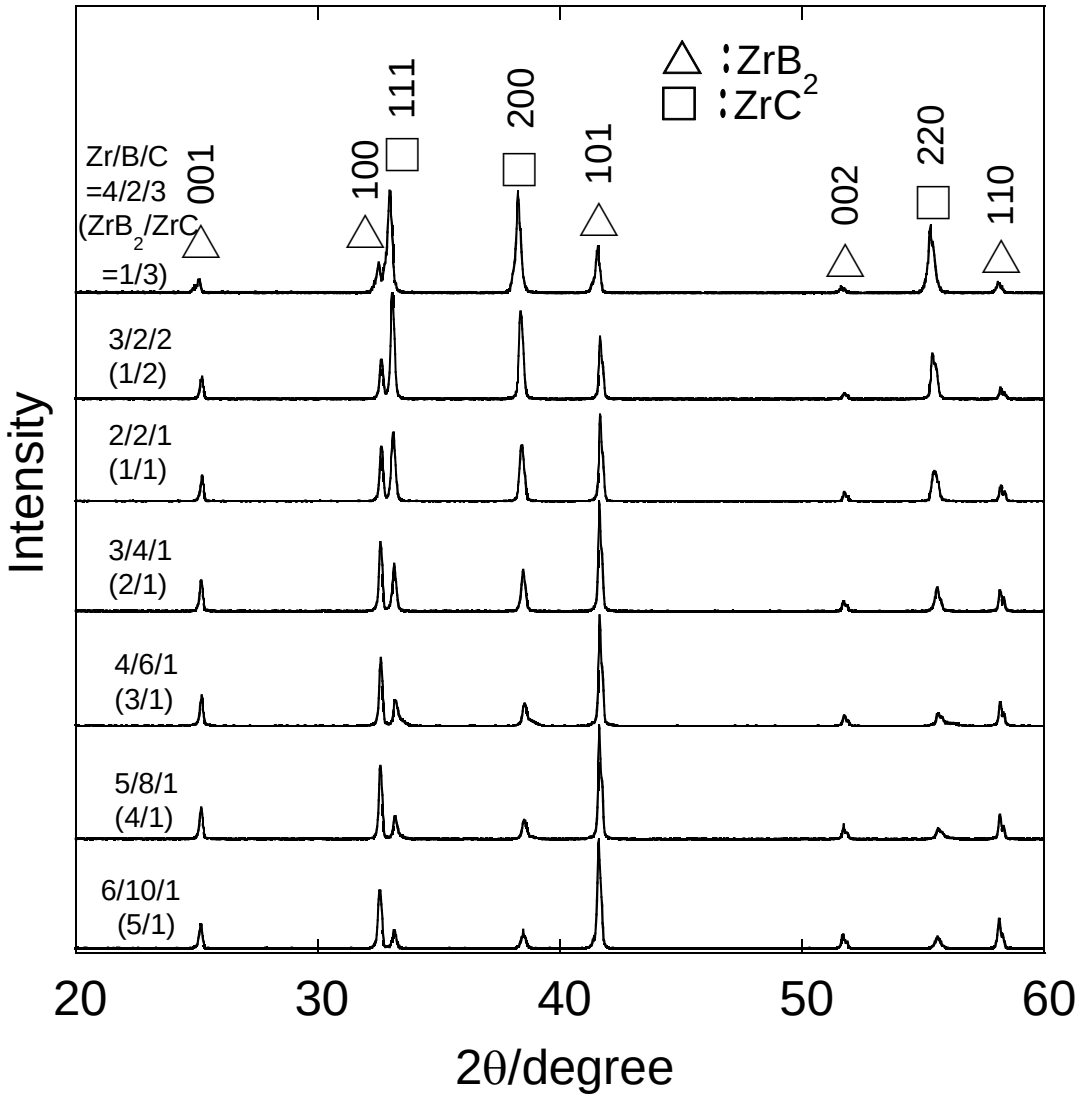
△ :ZrB2
□ :ZrC
001
100
111
200
101
002
220
110
Zr/B/C
=4/2/3
(ZrB2/ZrC
=1/3)
3/2/2
(1/2)
2/2/1
(1/1)
3/4/1
(2/1)
4/6/1
(3/1)
5/8/1
(4/1)
6/10/1
(5/1)
Intensity
20
30
40
50
60
2θ/degree

Fig.2

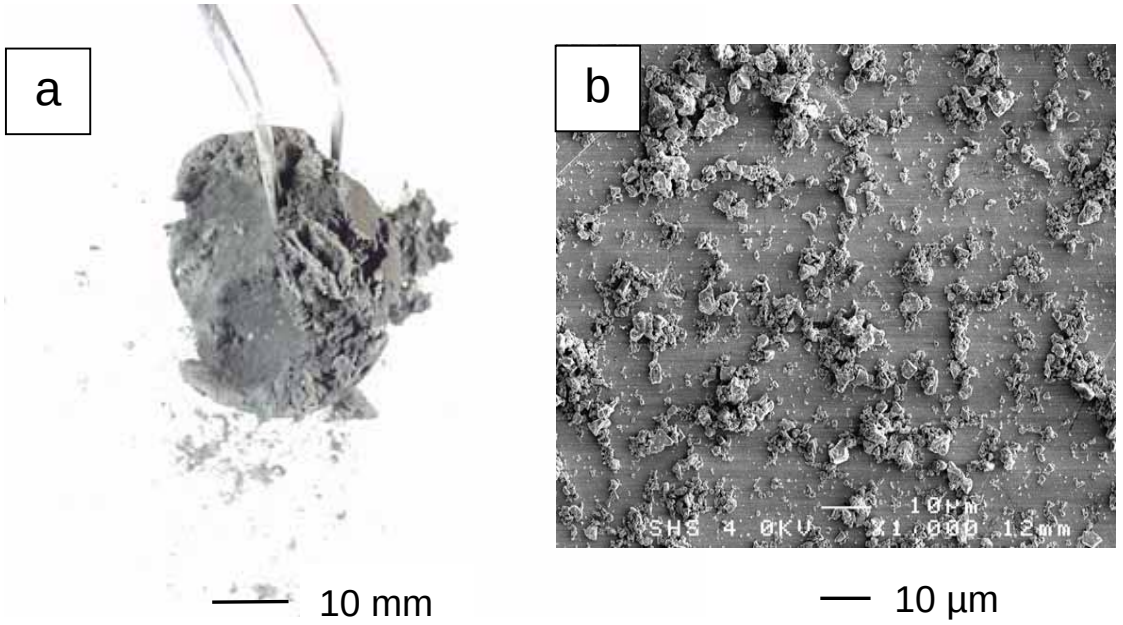

Fig.3

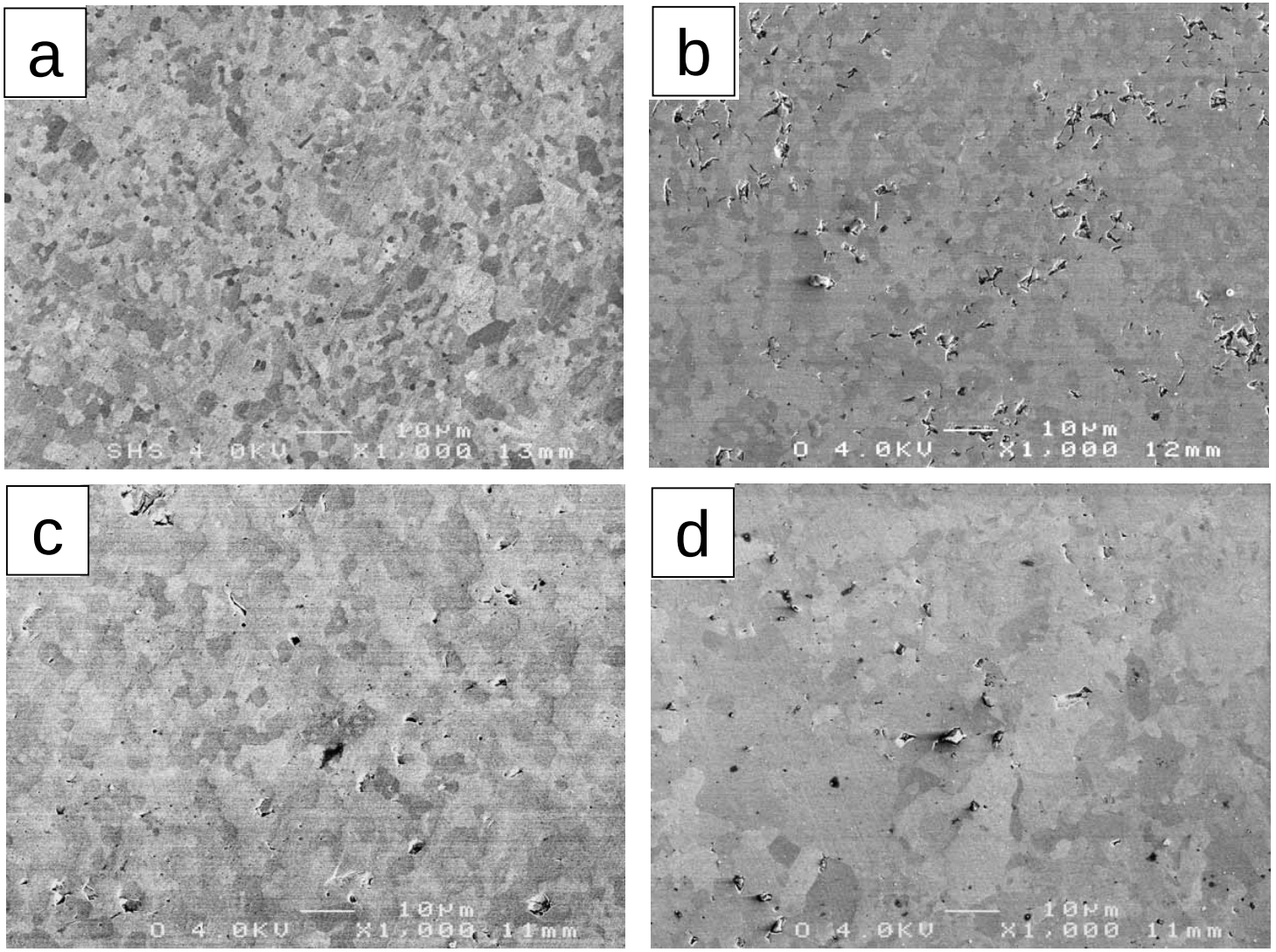
a
10μm
SHS 4.0KV X1,000 13mm
b
10μm
0 4.0KV X1,000 12mm
c
10μm
0 4.0KV X1,000 11mm
d
10μm
0 4.0KV X1,000 11mm
— 10 μm

Fig.4

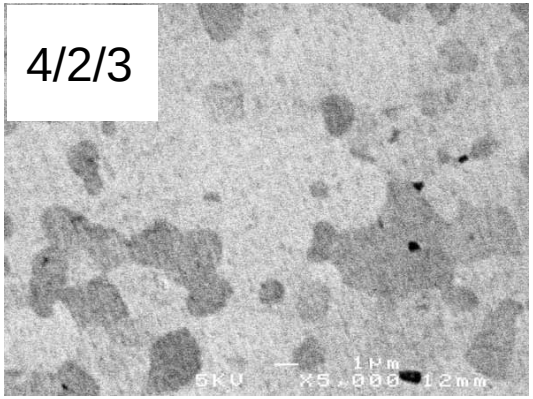
4/2/3
1μm
5KV X5,000 12mm

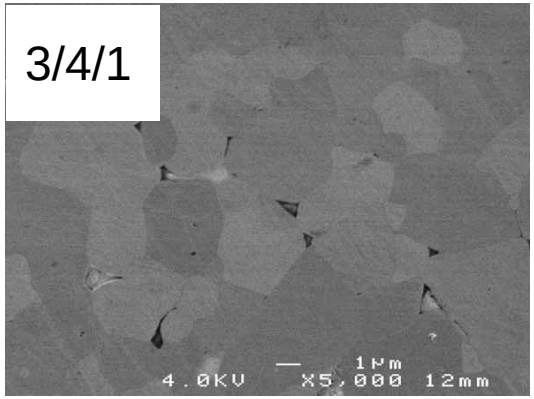
3/4/1
1μm
4.0KV X5,000 12mm

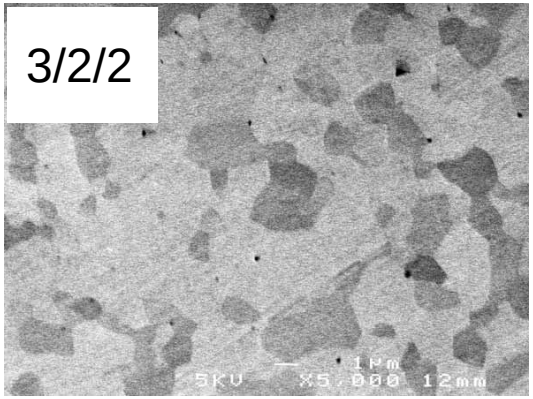
3/2/2
1μm
5KV X5,000 12mm

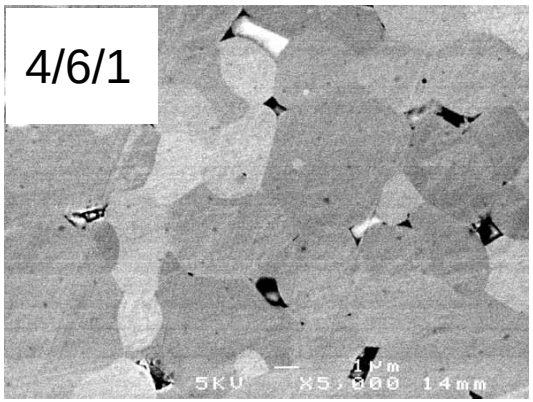
4/6/1
1μm
5KV X5,000 14mm

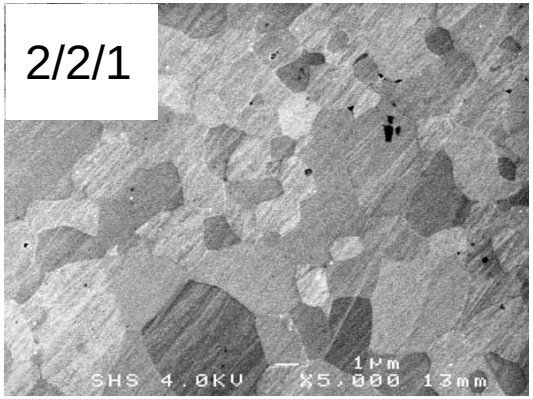
2/2/1
1μm
SHS 4.0KV X5,000 13mm

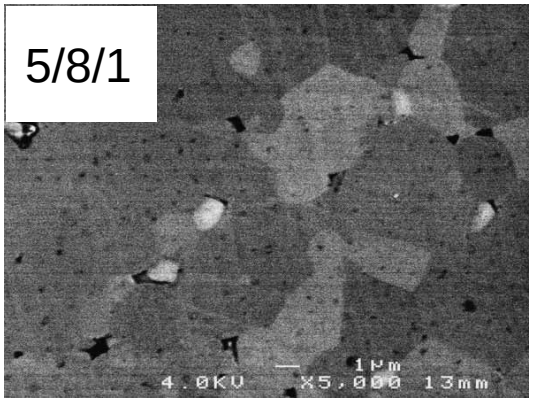
5/8/1
1μm
4.0KV X5,000 13mm

– 1 μm

Sintered samples	Vickers hardness, HV (GPa)	Fracture toughness, K_C (MPa·$m^{1/2}$)*	Relative density (%)
MA-SHS powder compact of Zr/B/C=2/2/1	17.8	3.8	98.5
MA powder compact of Zr/B/C=2/2/1	13.8	4.5	97.2
Mixing powder compact of Zr/B/C=2/2/1	13.7	3.8	96.9
Commercial powder compact of ZrB_2/ZrC=1/1	16.6	3.4	97.6

*) calculated according to JIS R1607, $K_C = 0.026(E^{1/2}P^{1/2}a/C^{3/2})$, where P is the indentation load, a the half-length of the indent, C the half length of the crack, and E the Young's modulus of the composite. (E=435 GPa was used as the mean of 470 GPa for ZrB_2 and 400 GPa for ZrC).

Table 1 The relative density and the mechanical properties of Vickers hardness, HV and fracture toughness, K_C of the MA-SHS, the MA, the mixing and the commercial powder compacts, which are described in detail in text.

Sintered samples	Vickers hardness, HV (GPa)	Fracture toughness, K_C (MPa·$m^{1/2}$)*	Relative density (%)
MA-SHS powder compact of Zr/B/C=4/2/3	17.5	3.0	97.6
MA-SHS powder compact of Zr/B/C=3/2/2	17.4	2.9	98.8
MA-SHS powder compact of Zr/B/C=2/2/1	17.8	3.8	98.5
MA-SHS powder compact of Zr/B/C=3/4/1	14.4	4.8	98.2
MA-SHS powder compact of Zr/B/C=4/6/1	14.5	5.1	98.4
MA-SHS powder compact of Zr/B/C=5/8/1	13.6	4.2	97.5

*) calculated according to JIS R1607, $K_C = 0.026(E^{1/2}P^{1/2}a/C^{3/2})$, where P is the indentation load, a the half-length of the indent, C the half length of the crack, and E the Young's modulus of the composite.

Table 2 The relative density and the mechanical properties of Vickers hardness, HV and fracture toughness, K_C of the SPS compacts obtained from the MA-SHS powders of Zr/B/C=4/2/3-5/8/1.